MATHEMATICAL MODELING OF MOLD-FILLING AND SOLIDIFICATION OF CASTINGS: PART II – APPLICATION TO A CU 5%ZN ALLOY CASTING IN A SAND MOLD

Pariona M. M. [1] , Bertelli F.[2], Cheung N.[2], Garcia A.[2]
[1] Department of Mathematics and Statistics, State University of Ponta Grossa, UEPG Campus Uvaranas, Block CIPP, Laboratory LIMAC, :84030900, Ponta Grossa, PR, Brazil
[2] Department of Materials Engineering, University of Campinas - UNICAMP, PO Box 6122, 13083-970, Campinas, SP, Brazil.

MATEMATICKÉ MODELOVANIE PLNENIA FORMY A TUHNUTIA ODLIATKOV ČASŤ II – APLIKÁCIA S POUŽITÍM ZLIATINY Cu-5%Zn

Pariona M. M. [1] , Bertelli F.[2], Cheung N.[2],Garcia A.[2]
[1] Department of Mathematics and Statistics, State University of Ponta Grossa, UEPG Campus Uvaranas, Block CIPP, Laboratory LIMAC, :84030900, Ponta Grossa, PR, Brazil
[2] Department of Materials Engineering, University of Campinas - UNICAMP, PO Box 6122, 13083-970, Campinas, SP, Brazil.

Abstrakt

V tejto práci bola uskutočnená matematická simulácia plnenia a tuhnutia zliatiny Cu-5%Zn s využitím metódy konečných prvkov. S cieľom uskutočnenia tejto práce boli využité metóda konečných prvkov a softwarový program ANSYS. Proces plnenia formy bol simulovaný pri atmosférických podmienkach pre gravitačné odlievanie a tekutý kov bol odlievaný do formy cez liaci kanál. Teplotné profily vytvorené v t = 3s počas procesu plnenia formy boli považované za hraničnú podmienku a všetky tepelno fyzikálne vlastnosti pre zliatinu a pre pieskovú formu boli považované za funkciu teploty. Simulácie tiež zohľadnili tri spôsoby uvoľnenia latentného tepla: lineárny, exponenciálny (Scheil) a sínusový priebeh ako funkciu tuhého podielu a analyzovaný bol ich vplyv na priebeh tuhnutia. Získané boli nasledujúce výsledky: rýchlosť, teplotná distribúcia, tlakové polia a tuhý podiel počas plnenia formy ; teplotné pole, tepelný tok, teplotné gradienty a ochladzovacie krivky v kove a vo forme počas tuhnutia. Výhoda uvedenej simulácie je analýza niekoľkých javov prítomných v procese plnenia formy , čo nie je jednoduché experimentálne vizualizovať a môže byť determinantou pre fázu tuhnutia.

Abstract

In this work, numerical simulations of mold-filling and solidification of a Cu-5%Zn alloy were performed by using a finite element technique. In order to accomplish this work, the finite-element technique and the ANSYS software program were used. The mold filling process was simulated in atmospheric conditions under gravity and the liquid metal was poured into the mold through a mold channel. The temperature profiles generated at t =3 s during the mold filling process was considered as a boundary condition and all the thermophysical properties for the alloy and for the sand mold were considered as a function of temperature. The simulations have also taken into account three forms of latent heat release: linear, exponential (Scheil) and sinusoid behavior as a function of the solid fraction, and their effects on the solidification

behavior were analyzed. The following results were obtained: velocity, temperature distribution, pressure fields and the solid fraction during mold-filling; and thermal field, heat flux, temperature gradients and cooling curves in the metal and in the mold during solidification. The advantage of the present simulation is to analyze several phenomena present in the mold filling process which is not trivial to be experimentally visualized, and can be determinant for the solidification stage.

Keywords: numerical simulation, finite-element method, mold-filling, solidification, Cu 5%Zn alloy

1. Introduction

Brasses are alloys of copper and zinc (generally from 5 to 40%Zn), and may contain small amounts of other alloying elements. Brass components are available in a range of forms, e.g.: heat exchangers, springs, car radiators, fasteners, hot formed parts, extruded sections, forgings, condenser tubes, architectural, sections, pressure tubing, bearings, bushes, ornamental features, gearwheels, and can be fabricated by casting, forging, stamping, rolling, extrusion and machining. These alloys can be classified in two categories; alpha alloys with less than 35% zinc which are ductile and can be cold worked and alpha/beta or duplex alloys which are harder and stronger with limited cold ductility. Lead can be added as an alloying element resulting in a brass that can be rapidly machined and produces minimal tool wear. Additions of aluminum, iron and manganese to brass improve strength, whilst silicon additions improve wear resistance. Additions of tin or aluminum to either alpha or duplex brasses improve corrosion resistance in sea and brackish waters for applications such as propellers [1].

In the second part of this paper, the numerical simulation of mold filling and solidification of the Cu-5%Zn alloy was accomplished in a sand mold. For this purpose, the finite-element method and the software ANSYS-FLOTRAN-CFD were applied. During the simulation of the mold filling stage, the properties such as density, specific heat and viscosity of the liquid alloy were considered as constants but the thermal conductivity was assumed to vary with the temperature. In addition, the turbulence, the gravity action and incompressible fluid were taken into account, and the time of mold filling was of 3 s. The following results were then determined: the flow velocity, the pressure variation, heat transfer both in the mold and in the ladle, and also the volumetric fraction parameter. One of the initial conditions for the solidification simulation, i. e., the thermal field, is furnished after the mold filling process, i. e., after 3 s. During simulation of solidification, thermophysical properties varying with the temperature for both the alloy and the mold material were considered. Three different latent heat release approaches were analyzed: a linear equation, Scheil's equation and the equation proposed by Radovic and Lalovic [2].

2. Methodology of the numerical simulation

The modeled geometry is represented in Figure 1. In this Figure we can observe that between the ladle exit and the mold entrance there is a free space of 0.1 m. Not only this free space but also the exit of the ladle is exposed to the environment. To reach the convergence according to the condition of the volume of Fluid (VOF) algorithm, the geometry of the mesh element should be of quadrilateral form and the mesh of the mold channel must have continuity, as shown in Figure 1.

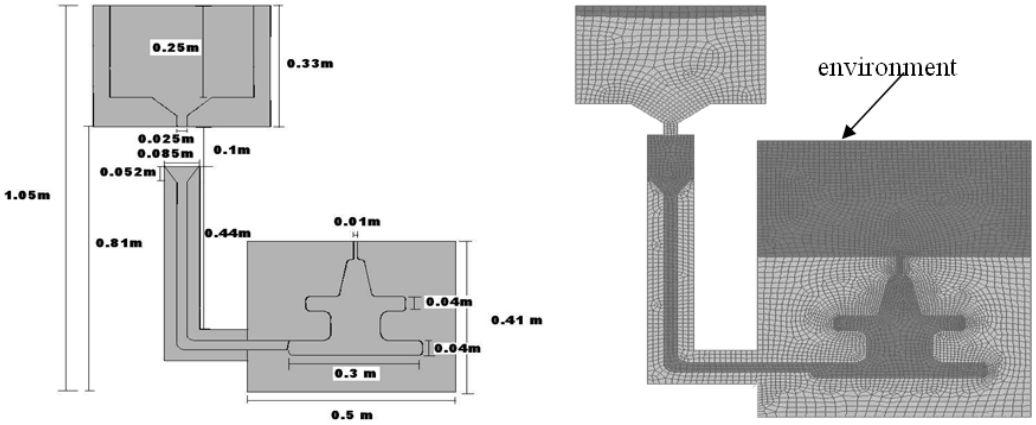

Fig.1 a) Ladle/ mold and casting geometries b) adopted mesh for 2-D simulation – dimensions in meters.

The properties of the liquid metal used in the mold filling simulations are listed in Table 1. In order to simulate the liquid metal flow inside the sand mold, the following conditions were considered: (a) the liquid metal and the sand mold were stabilized in normal condition of atmospheric pressure; (b) the initial temperature of the liquid metal was of 1550 K and the mold temperature was considered to be equal to that of the environment; (c) the velocity of the liquid was fastened in zero on the mold walls; (d) the mathematical model for the turbulence New κ-ε Model [3] was considered. The constants for this model are shown in Table 2; (e) the VOF algorithm was used for mold filling. A strategy in the VOF technique was applied to describe the mold wall as a region not allowed to be filled by the liquid: The VOF for the mold wall was considered 1 (light gray color). According to Figure (1 b), the dark gray color regions represent the places that could be filled by the liquid and their VOF values are 0. In this sense, during the dynamics of filling, the color of the mold cavity gradually becomes light gray color (VOF=1), i. e., the same color of the mold wall; (f) the total time for mold filling was of 3 s and the step time was of 0.05 s (g) the number of iterations by step was 30; (j) the properties of the materials were informed and the mesh of the model was made; and (k) a 2-D solution was considered.

Table 1 Properties of the Cu5%Zn alloy for the mold-filling process at 1354 K [4]

Density (Kg/m^3)	Specific heat (J/Kg.K)	Viscosity (Pa.s)
7857.143	492.8571	0.0034

Table 2 NKE turbulence model coefficients adopted in this article [7]

C_1	C_2	σ_k	σ_ε	σ_t	C_3	C_4	C_{1M}	β_1
1.44	1.92	1.0	1.2	0.85	1.0	0.	0.43	0.0

To accomplish the solution process of Equations (1)-(6) described in part I of the present study, the finite-element method and the software ANSYS-FLOTRAN-CFD [5] were used. Specific heat and viscosity were considered constants and incompressible fluid condition was assumed. The most appropriate technique considered to generate the pressure field was the Preconditioned Conjugate Residual Method and for the velocity, it was the Tri-diagonal Matrix

Algorithm [5]. The convergence in each iteration was controlled through the norm of the solution parameters, as suggested in the literature [5,6].

After the mold-filling step was complete, the solidification step starts. Firstly, the meshes of casting and mold in 2D were made. After that, the thermophysical properties of the alloy (Table 3) and of the green sand mold (Table 4) as a function of temperature were incorporated (density, specific heat and thermal conductivity). The following boundary conditions were considered: the temperature field after 3 s of mold-filling, the ambient surface convection heat transfer coefficient (h= 70 $W/m^2.K$ at $T\infty$ =297 K) applied at the outer mold surface and the heat generation given by the models I (Eq. 10); II (Eq. 11) and III (Eq. 12) described in Part I of the present study. The initial temperature of the mold was considered to be 293 K and the liquidus temperature of the alloy is 1354 K according to the Cu - Zn phase

Table 3 Properties of Cu5%Zn alloy [4]

Temperature (K)	Specific heat (J/Kg.K)	Temperature (K)	Density (Kg/m^3)	Temperature (K)	Thermal conductivity (W/m.k)
1273.000	466.071	1273.000	8344.642	1273.000	321.428
1284.718	466.071	1284.718	8344.642	1284.538	321.428
1296.437	466.071	1296.437	8344.642	1296.077	321.428
1308.156	467.857	1308.156	8344.642	1307.615	321.428
1315.187	467.857	1317.531	8344.642	1319.154	321.428
1319.875	469.642	1322.219	8275.000	1321.462	314.285
1324.562	471.428	1326.906	8251.786	1323.769	307.143
1329.250	471.428	1331.594	8158.928	1326.077	300.000
1333.937	478.571	1336.281	8019.643	1328.385	292.857
1338.625	491.071	1340.968	7857.143	1330.692	278.571
1355.031	492.857	1355.031	7857.143	1333.000	257.143
1366.750	492.857	1366.750	7857.143	1335.308	228.571
1378.468	492.857	1378.468	7845.535	1337.615	178.571
1390.187	492.857	1390.187	7833.928	1342.231	107.143
1401.906	492.857	1401.906	7833.928	1376.846	107.143
1413.625	492.857	1413.625	7833.928	11399.923	107.143
1423.000	492.857	1423.000	7810.714	1423.000	107.143
Latent heat = 193000 J/kg					

Table 4 Properties of green sand mold materials [7]

Temperature (K)	Density (Kg/m^3)	Temperature (K)	Specific heat (J/Kg.K)	Temperature (K)	Thermal conductivity (W/m.k)
295	1488	373	1118	373	0.785
373	1482	473	1114	473	0.732
473	1475	573	1160	573	0.693
573	1468	673	1178	673	0.668
673	1462	773	1196	773	0.66
773	1456	873	1214	873	0.668
873	1448	973	1232	973	0.691
973	1442	1073	1250	1073	0.733
1073	1437	1173	1268	1173	0.79
1173	1433	1273	1285	1273	0.863
1273	1428	1373	1303	1373	0.951
1373	1422	1473	1321	1473	1.054
1473	1417	1573	1339	1573	1.175
1573	1413	1673	1356	1673	1.303
1673	1401	1773	1374	1773	1.439
1773	1382	1873	1392	1873	1.582
1873	1360				

diagram. The equilibrium partition coefficient was considered to be 0.12. The total time of cooling was 5400 s, time step size was of 0.005 s, minimum time step was of 0.001s and the maximum time-step was of 100s to reach the convergence according to the suggestion of Babaei et al. [6].

3. Results and discussion

Different parameters characterizing the mold filling process were determined. These parameters were calculated for mold filling times of 1, 2 and 3 seconds. In Figure 2 the results of the instantaneous fluid velocity (m/s) are shown both in numerical values and in vectorial form. It is observed that the velocity varies as a function of the pathlines, being higher on the first second. It can also be observed that the fluid leaves out the mold. For 1s and 2s, high turbulence is noticed in the curvatures of the geometry, shown by the streamlines produced in Fig 2 in vectorial form. When the liquid is liberated from the mold at t = 2 s, an abrupt exit of fluid occurs and for t = 3 s the mold is completely filled and some molten metal flow through the mold exit. This phenomenon, of liquid exit as a form of jet, happens due to the abrupt variation of pressure, because the variation from high pressure to the atmospheric pressure. Therefore, in the next seconds, the liquid starts to slide on the external mold surface. The liquid turbulence was better reproduced in this work by the turbulence model N $\kappa-\varepsilon$ [5]. Other turbulence models were applied, but they did not succeed in reproducing the phenomenon adequately. In the literature concerning mold filling, the N $\kappa-\varepsilon$ model used by the Ansys was not found, but, the model $\kappa-\varepsilon$ was found [8-13].

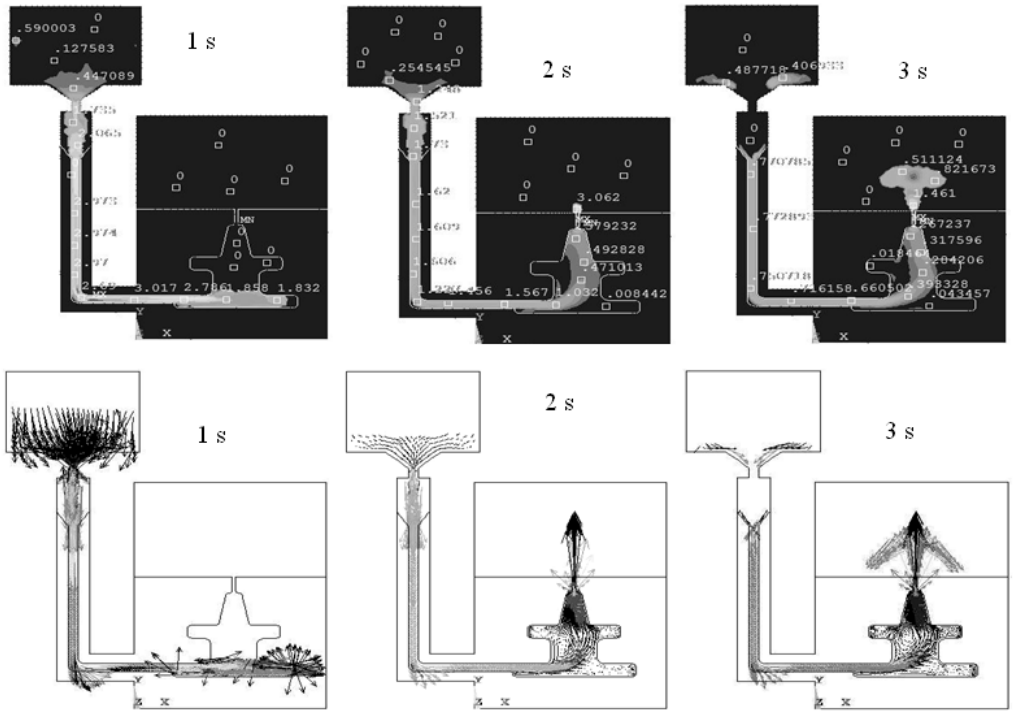

Fig.2 Velocity (m/s) variation in magnitude and vectorial forms during mold filling: t = 1; 2 and 3 s

In Figure 3 the pressure variation is shown in the gate and in the mold. In the first second a maximum pressure of 139732 Pa is shown to be located at the sprue base. For t = 2 s there is a maximum pressure of 138005 Pa at the right inferior part of the mold. For t = 3 s, at the same point of the mold previously considered for t =2 s, the pressure lowers to 134280 Pa. The largest pressure variation is observed for the time of t =2 s. As the liquid metal is being cooled, for t= 3 s the pressure in the mold decreases.

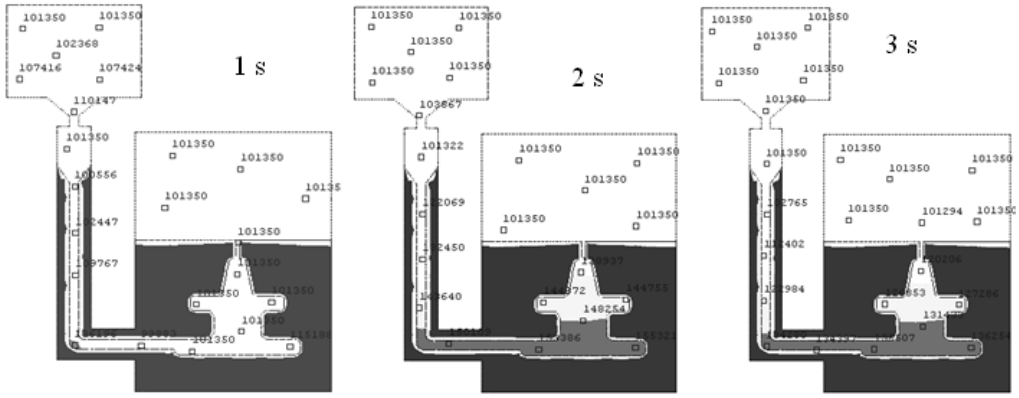

Fig.3 Pressure (atm) variation during mold filling: t = 1; 2 and 3 s

Another result calculated in this study was the temperature variation during mold filling, as shown in Figure 4. It is observed that the temperature is approximately constant inside the gate and at the inferior part of the mold. On the other hand, in other regions inside the mold, the temperature decreases to about 200 K. In a general way, in all the mold curvatures where fluid stagnation occurs, an appreciable cooling is shown. For instance, from t = 1s to 2s, a decrease of about 400 K in the temperature at the right inferior part of the mold can be observed. For t = 3 s, the simulation has shown that the liquid jet encountered a free pathline from the ladle to the mold exit and as shown in Figure 4, the liquid did not fill the lateral cavities of the mold, avoiding turbulence. In this sense, the heat losses caused by convection effects can be neglected and due to this fact, the fluid expelled from the mold has a high temperature, which is close to the pouring temperature (1550 K).

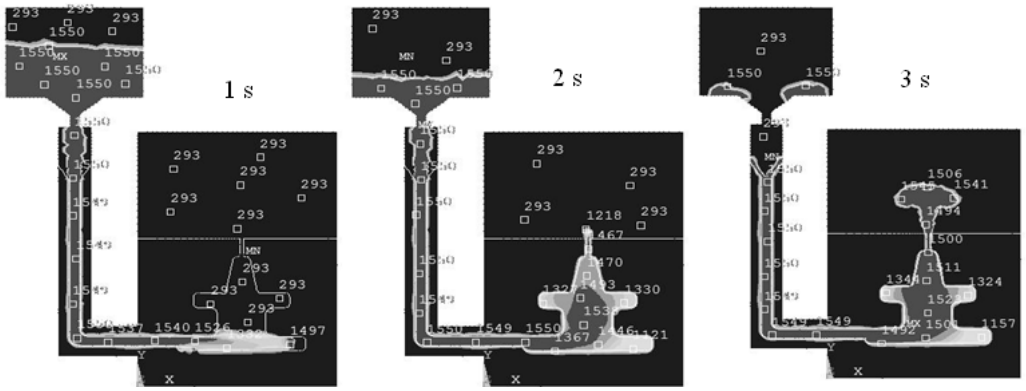

Fig.4 Temperature (K) variation during mold filling: t = 1; 2 and 3 s

The volumetric fraction was calculated, as it is shown in Figure 5, where the gray color represents the cell completely filled by the liquid and it is characterized by the value of unity (1), the black color represents the cell completely empty and it is characterized with the value of zero (0) and the gray clear color represents the cell during the filling process and it is characterized by values between zero and unity. For t =1 s some empty areas and filled areas can be observed; for t =2 s there are still some areas being filled and for t =3 s a uniform filled pattern can be observed in the whole volume of the mold and a drop came out from the mold.

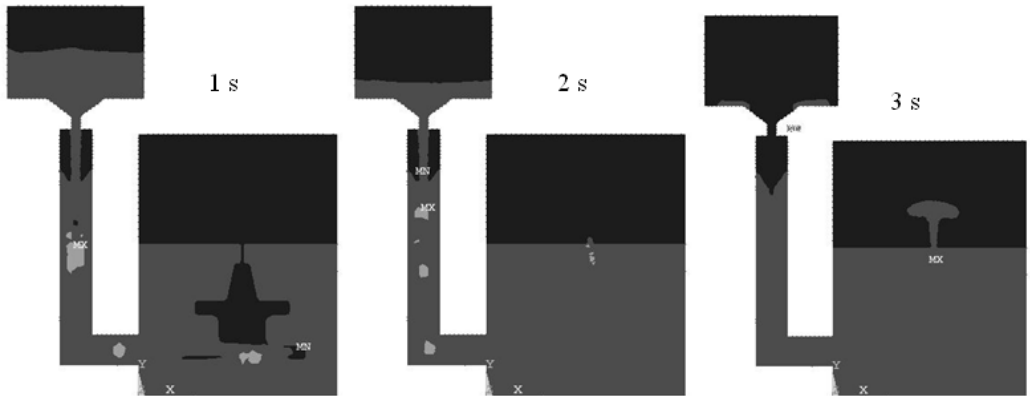

Fig.5 Volume fraction during mold filling: t = 1; 2 and 3 s

Macrostructural defects, such as shrinkage, macrosegregation, mold erosion, etc, [14, 15] depend on the way the mold is filled, on the quality of the fluid flow in the mold cavity, on the height of the ladle in relation to the mold, on the turbulence, on the melt superheat, on the filling velocity, on the surface tension, on the initial condition of pressure and temperature inside the mold and on the turbulence model. The volumetric fraction is an important parameter that characterizes the mold filling quality.

The solidification results can be seen in both qualitative and quantitative forms after t = 5400 s from the beginning of the cooling process. In Figure 6 the thermal field is shown in the whole system (left side) and in the casting (right side) for the three models of latent heat release used in simulations. It can be observed that the thermal field results are different for each heat generation approach. Model I has presented the higher thermal field when compared to the other two approaches, followed by model III and then for model II. This means that the cooling process is slower for model I than for the other models. For all the cases examined the largest and lowest temperatures occurred at the mold entrance and mold exit, respectively, as it was expected. The heat flux is shown in Figure 10 (left side), being larger for model I, followed by model III and finally by model II. The heat flux is the highest at regions where the cooling conditions were the best, i.e., at the mold exit, and is smaller at areas of fluid stagnation (curved parts of the casting geometry). Figure 7(right side) also shows the results of temperature gradients, which are higher for model I, followed by model III and finally by model II. The temperature gradient is also highest at areas of best cooling, conditions for example, at the mold exit.

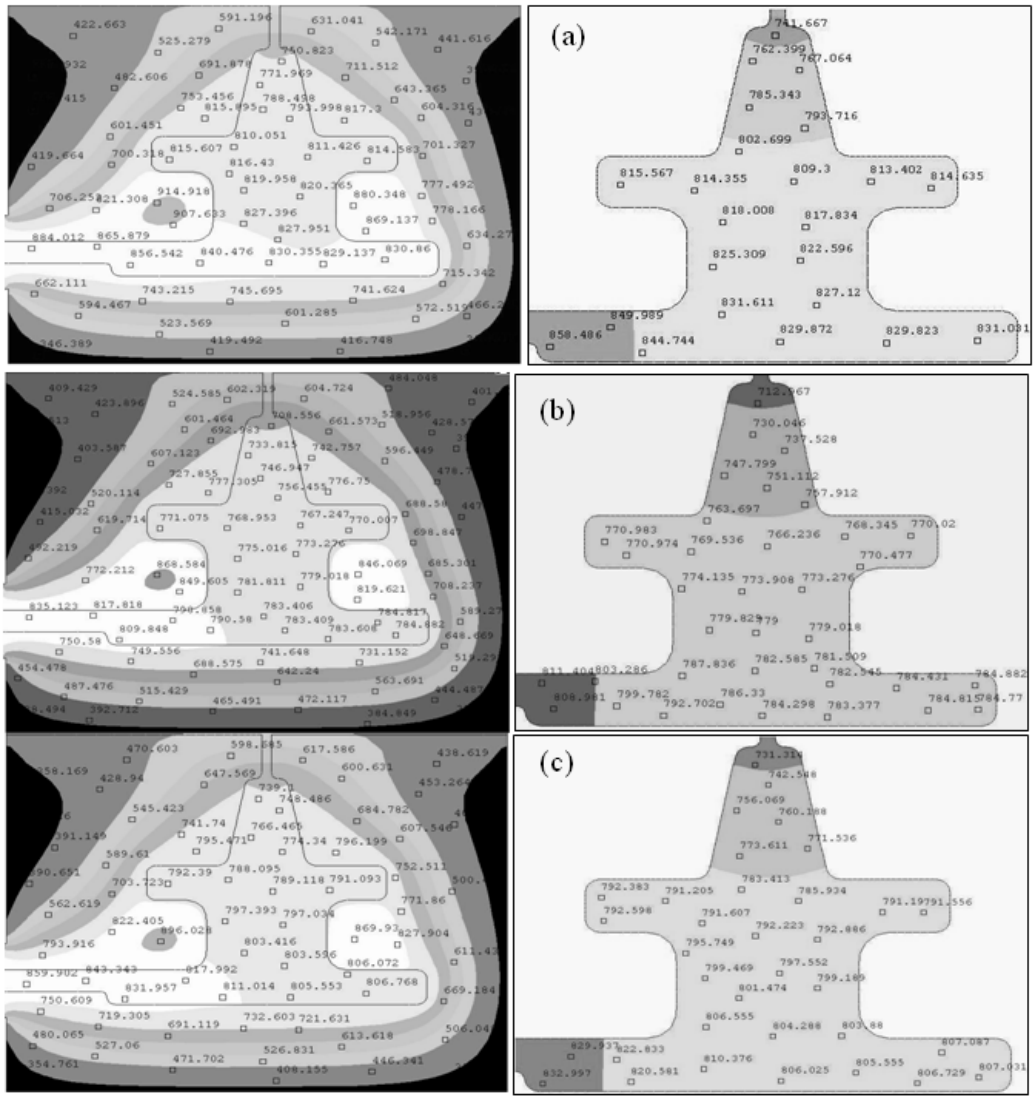

Fig.6 Thermal field in the metal/mold system (left) and in casting (right): (a) for model I, (b) for model II and (c) for model III

Other important results from the present study were the casting cooling curves and the mold heating/cooling curves. These results were obtained for different positions along the casting and in the mold (Fig. 8). In Figure 9, the left side represents the cooling curves in the casting, and the right side represents the heating/cooling curves in the mold. It is observed that at some points of Figure 8, up to two curvature changes have occurred and it is known that such behavior is connected to a phase change. Figure 10 (a) shows a comparison of temperature evolution at position (1) for the three formulations of latent heat release: linear (model I), Scheil (model (II) and Radovic and Lalovic (model III). It can be observed that the highest temperature profile corresponds to model I, followed by model III and last by model II, mainly after the solidification range. Although not presented, a similar behavior has occurred at other positions

in the casting. Chen and Tsai [16] analyzed theoretically four different modes of latent heat release for two of alloys solidified in sand molds: Al-4,5wt% Cu (wide mushy region, 136K) and a 1wt% Cr steel alloy (narrow mushy region, 33.3K). In their work, they conclude that no significant differences can be observed in the casting temperature for different modes of latent heat release, when the alloy mushy zone is narrow. The alloy used in the present work, Cu-5wt%Zn, according to its phase diagram, has a narrow mushy zone (less than 10K). Figure (10) shows that there is a significant temperature profile difference due to the use of the three

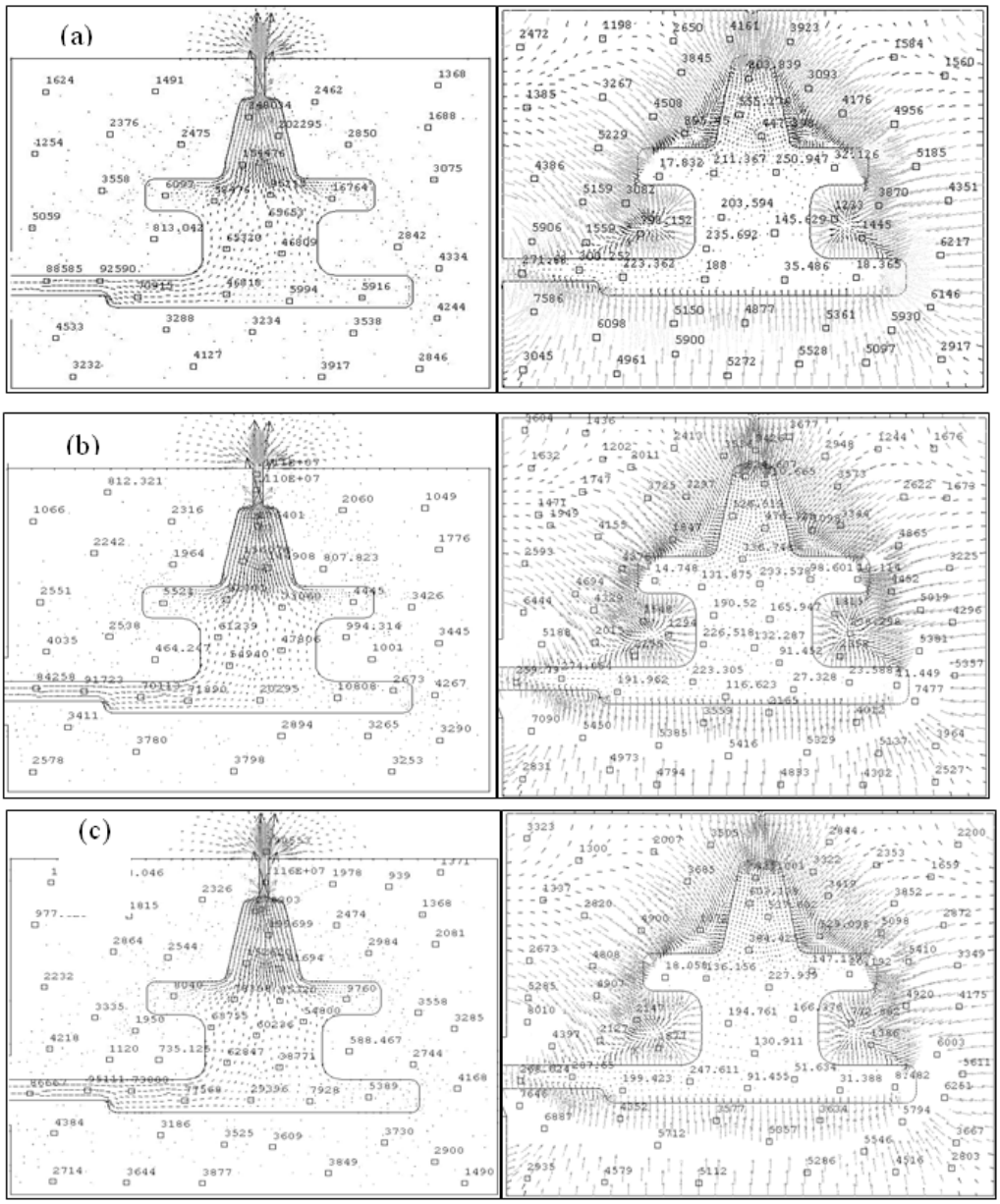

Fig.7 Heat flux (left) (W/m^2) and temperature gradient (right) (K/m) in casting: (a) for model I, (b) for model II and (c) for model III

different latent heat release approaches. Probably, the divergent conclusion in relation to Chen and Tsai work is due to the fact that their model does not take into account fluid motion. This fact permits to affirm that fluid mechanics plays an important role during solidification. In addition, it is important to remark that the latent heat release form has strongly influenced the local solidification time. Such solidification parameter affects the microstructure characterized by primary and secondary dendritic arm spacings. Correlations between dendritic spacing and local time solidification (t_{SL}) are well known in the literature [17]. Investigations correlating ultimate tensile strength (σ_U) and secondary (SDAS) or primary (PDAS) dendrite arm spacings have shown that (σ_U) increases with decreasing (SDAS) or(PDAS) [17,18].

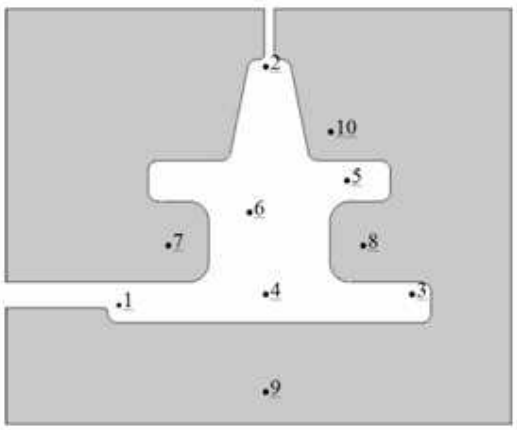

Fig.8 Reference points in the mold and in the casting

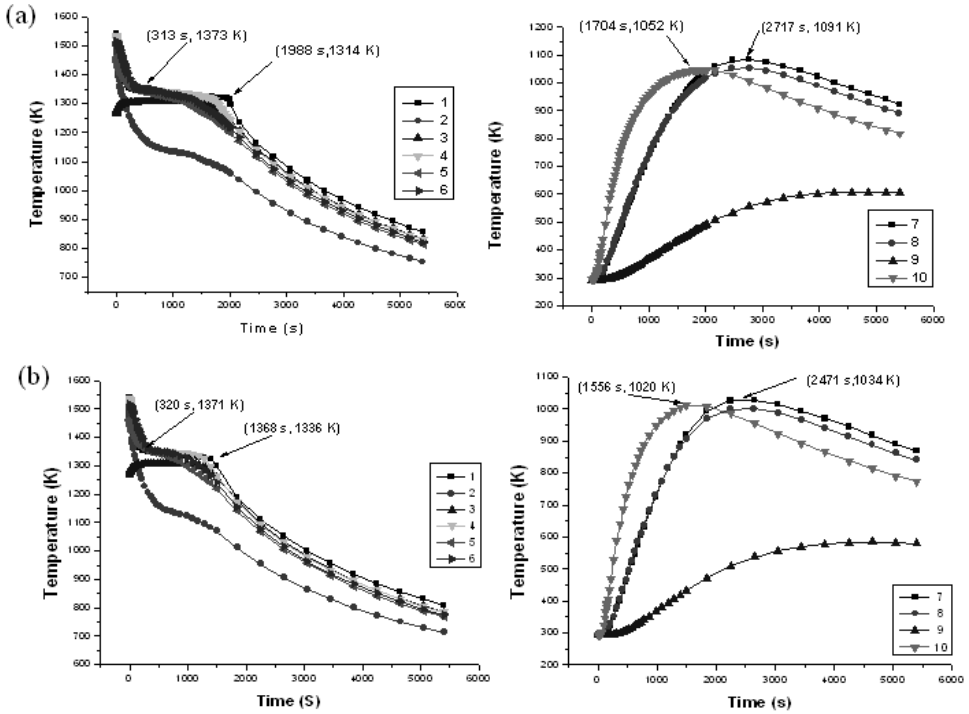

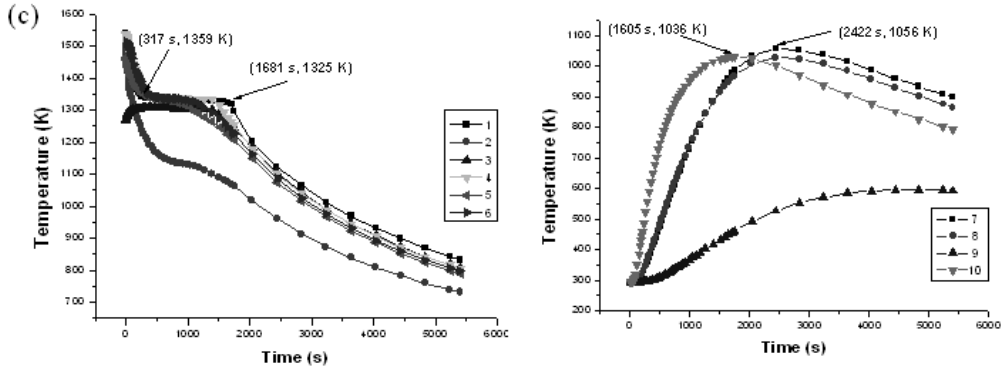

Fig.9 Cooling curves in casting (left), and heating and/or cooling curves in sand mold (a) for model I, (b) for model II and (c) for model III

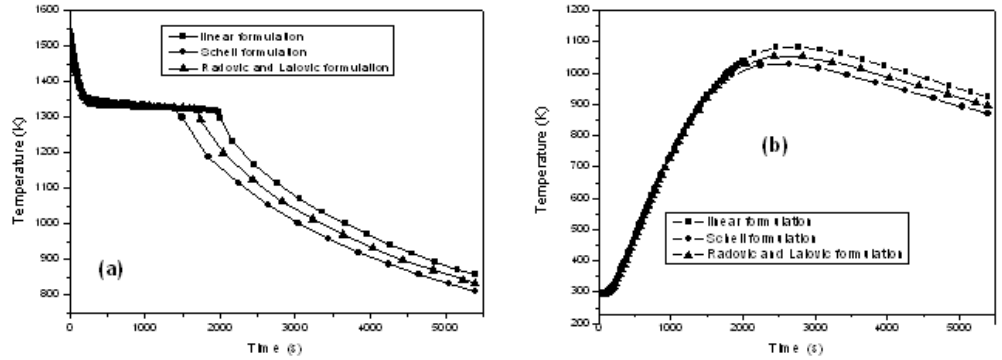

Fig.10 Comparison of three latent heat release formulations for position (1)

The heating/cooling curves that correspond to points 7 and 10 inside the sand mold were more prominent, because these points are closer to the casting. Figure 10 (b) shows a comparison of temperature evolution at position (7) for the three formulations of latent heat release. It can be observed again, that the highest temperature profile corresponds to model I, followed by model III and last by model II, and this behavior is repeated for other positions in the mold.

The research of mold-filling and solidification by simulation in castings is a complex work, because it involves the presence of many phenomena that occur simultaneously. The knowledge and control of all parameters involved in these phenomena is very important and challenging with a view to obtain high-quality castings. The mold-filling quality certainly influences solidification since macro and microstructural defects can be produced during the filling stage and, consequently, affects the casting final quality.

4. Conclusions

The following major conclusions can be drawn from the numerical analysis carried out in the present study: The VOF method has proved to be a powerful technique, for the control of mold filling. The simulation process operates connected with the solutions of the Navier-Stokes and the VOF equations. The mold-filling quality certainly influences solidification since

macro and microstructural defects can be produced during the filling stage and, consequently, affects the casting final quality.

The three latent heat release forms implemented into the model resulted in significant different thermal responses, which is in contradiction with a previous report in the literature.

The finite element method has proved to be a powerful mathematical tool to analyze mold-filling and solidification, which are not trivial to visualize experimentally. The simulation permits to visualize the filling dynamics, the cooling stage and to control the process by varying the operational parameters. For the sake of competitiveness in the world market, the practice of simulation and mathematical modeling in casting industry can produce a series of benefits such as optimization, time saving, waste minimization, and improvement on casting final quality.

Acknowledgements

The authors acknowledge financial support provided by CNPq (The Brazilian Research Council), FAPESP (The Scientific Research Foundation of the State of São Paulo, Brazil) and CAPES - Coordenação de Aperfeiçoamento de Pessoal de Nível Superior.

Literature

[1] Callister Jr., W. D., Materials Science and Engineering – An Introduction, John Wiley and Sons, New York, 1994.
[2] Radovic Z., Lalovic M.: Journal of Materials Processing Technology, vol.160, 2005, pp.156–159.
[3] Son G., Dhi V.K.: International Journal of Heat and Mass Transfer, vol.51, 2008, pp.1156–1167.
[4] Miettinen J.: Computational Materials Science, vol.22, 2001, pp.240-260.
[5] Handbook Ansys. 2008 Inc. Canonsburg, PA.
[6] Babaei R., Abdollahi J., Homayonifar P., Varahram N., Davami P.: Computer Methods in Applied Mechanics and Engineering, vol.195, 2006, pp.775–795.
[7] Midea T. and Shah J.V.: AFS Transaction, vol.02-080, 2002, pp.1-16.
[8] Zaidi K., Abbes B., Teodosiu C.: Computer Methods in Applied Mechanics and Engineering, vol.144, 1997, pp.227-233.
[9] Aboutalebi M.R., Guthrie R.I.L., Seyedein S.H.: Applied Mathematical Modelling, vol.31, 2007, pp.1671–1689.
[10] Cheng T.S., Yang W.J.: Computers & Fluids, vol.37, 2008, pp.194–206.
[11] Sharma A.K., Velusamy K. Balaji C.: Annals of Nuclear Energy. vol.35, 2008, pp.1502-1514.
[12] Ha M.Y., Lee H.G., Seong S.H.: Journal of Materials processing Technology, vol.133, 2003, pp.322-339.
[13] Pericleous K., Bojarevics V., Djambazov G., Harding R.A., Wickins M.: Applied Mathematical Modelling, vol.30, 2006, pp.1262–1280.
[14] Im I.-T., Kim W.-S., Lee K.-S.: International Journal of Heat and Mass Transfer, vol.44, 2001, pp.1507-1515.
[15] Hirt C.W., Nichols B.D.: Journal of Computational Physics, vol. 39, 1981, pp. 201-225.
[16] Chen J. H., Tsai H. L.: AFS Transactions, 1990, pp. 539-546.
[17] Goulart P. R., Spinelli J. E., Osório W. R., Garcia A.: Materials Science and Engineering, vol A 421, 2006, pp. 245-253.
[18] Quaresma J. M. V., Santos C. A., Garcia A.: Metallurgical and Materials Transactions A, vol. 31A, 2000, pp. 3167- 3177.